International Journal of Medical Toxicology & Legal Medicine Volume 27, No. 2, 2024
e-ISSN: 0974-4614
p-ISSN: 0972-0448

ROISegNet: A Novel Deep Learning Model for Automatic ROI Segmentation in Breast Thermogram Imagery

Preethi Veerlapalli[1], Sushama Rani Dutta[2]

[1]Research Scholar, Department of Computer Science and Engineering, Koneru Lakshmaiah Education Foundation, Hyderabad-500075, Telangana, India, Email: preethireddyveerlapalli@gmail.com
[2]Associate Professor, Department of Computer Science and Engineering, Koneru Lakshmaiah Education Foundation, Hyderabad-500075, Telangana, India, Email: sushamarani.dutta@klh.edu.in

Received: 16.08.2024 Revised: 19.09.2024 Accepted: 20.10.2024

ABSTRACT
Breast cancer is a leading cause of death for women worldwide. Breast thermography, a non-invasive imaging technique, can detect breast irregularities that may lead to breast cancer in the long run. Early identification of the risk of breast cancer can potentially prevent the disease and save lives. AI has emerged as a technological breakthrough in the healthcare sector and can be used with breast thermography and deep learning (DL) techniques for early breast cancer diagnosis.This study uses DL for breast region of interest (ROI) segmentation to facilitate breast cancer screening. Semantic segmentation using the atrous convolution DL model can effectively separate the ROI from breast thermography images. The deep learning system, ROISegNet, includes a decoder module that utilizes atrous convolution in the encoder, enhancing the efficiency of semantic segmentation. The framework's realization is demonstrated through an algorithm called Intelligent Segmentation of Breast ROI (ISBROI). According to our empirical investigation using the benchmark dataset DMR-IR, ROISegNet achieved a maximum accuracy of 98.63%, outperforming other models such as VGG19, ResNet50, InceptionV3, and Atrous Convolution.

Keywords: DL, ML, Breast Cancer, Atrous Convolution, ROISegNet (RSN), CSSA,mammography

1. INTRODUCTION

BC is among the most prevalent cancers among women diagnosed globally [1]. Currently, about 15% of all cancer-related fatalities in women are due to BC [2]. Breast disorders can be identified using imaging techniques, medical specialists, and self-examination. A biopsy is the sole method available to ascertain whether cancer is present or not [4]. These days, a variety of procedures for imaging, like ultrasound and mammography, are employed to detect BC at an early stage. Because mammography is inexpensive, highly detectable, and produces reliable findings, it is the most widely utilized screening modality. Breast cancer may be detected and classified using mammograms, an exact imaging method. It is known to function badly in a few cases, though, especially in those with dense breast tissue. Adolescent females may also suffer from severe side effects from ionizing radiation. In addition, mammography is known to have trouble detecting tumors smaller than 2 mm.These disadvantages have led to much interest in thermography, a recently discovered BC screening technique. Thermography is an inexpensive, non-invasive, radiation-free, and exclusive method [2]. As such, it can be used to identify young women and those with big breasts who have early-stage BC.

The fundamental idea of thermography is that anything organic emits IR radiation above zero degrees Celsius. IR radiation is converted into electrical impulses by an infrared thermal camera used for breast thermography. The result is a thermogram. Potential anomalies are brought to light by their temperature scale, which distinguishes them from normal tissue [17]. Breast thermography is more advantageous than mammography, including breast tissue thickness compatibility, comfort for male patients, and effectiveness across all age groups. Since thermography is renowned for being quick, secure, and precise, BC can be identified early.Segmenting the breast tissue is a crucial step in detecting BC. It is a technique for distinguishing, in thermal imaging, the breasts about other bodily parts [16]. To the greatest extent feasible, the excised area should contain every breast tissue, lobule, lymph node, and duct. Breast segmentation can be carried out fully automatically or entirely manually. Since each breast is amorphous and these images lack defined borders, most scientific research chooses to remove the breast area extraction operation manually or through a semi-automated process.

The last few decades have seen a focus on ML methods for thermography-based BC diagnosis; some researchers have studied tumor location and size, while others have studied features like breast quadrants and collection methods. Multilayer CNN are used in ML techniques such as deep learning. Deep learning may

automatically extract a training dataset's features [18]. With encouraging findings, researchers have recently employed CNNs to identify BC. CNNs were not commonly used in the past for the thermal imaging-based BC diagnosis procedure, Possibly because they are less efficient or have a higher computational weight than textural or statistical features [3]. One of the greatest approaches for pattern recognition nowadays is thought to be CNNs.

During training, the thermal imaging features used as noise in CNN models show the neck, shoulder, chess piece, and other extraneous body components. Pictures from thermography are challenging to understand because of their low spatial resolution. Because the segmentation results greatly influence the outcome of the classification procedure, it is imperative to identify the breast region in the thermal pictures. BC is one of the leading causes of death for females, as was previously established. Early detection is, therefore, essential to save lives. The radiology's interpretation of the thermogram determines the diagnostic effectiveness of thermography imaging, which uses infrared technology to discover breast cancer. As far as we know, there are several issues with the earlier work. These consist of (1) dataset limitations, (2) related work studies that excluded certain parts of the breast from segmentation models,(3) segmentation models with (4) investigations evaluating their model based just on the accuracy score, and a manual exclusion of the breast region. Nevertheless, If the dataset is unbalanced, a high accuracy rate does not guarantee that the model can distinguish between every class. Our research primarily focuses on thermal imaging-based breast region segmentation. According to the literature review, breast ROI segmentation utilizing DL and encoder-decoder architecture has not been the subject of significant research. We have provided the goods listed below.

1. To automatically segment the ROI from breast thermogram imaging, we suggested a deep learning system called ROISegNet. Our method leverages efficiency in semantic segmentation by designing a decoder module and using atrous convolution as part of the encoder.
2. We proposed an algorithm called Intelligent Segmentation of Breast ROI (ISBROI).
3. We created an application to evaluate ROISegNet. Our empirical analysis using the benchmark dataset DMR-IR shows thatROISegNet performs better than other models, including VGG19, ResNet50, InceptionV3, and Atrous Convolution.

The remaining portion of the job is organized as follows: Section 2 summarizes earlier studies andoffers semantic image segmentation for breast thermal pictures. Section 3 presents our method and underlying framework. Section 4 displays the results of our empirical investigation. Section 6 concludes ourstudy.

2. RELATED WORK

Previous studies on thermal image-based breast segmentation for BC detection are reviewed in this section. A novel thermography method that detects breast cancer by combining infrared pictures and machine learning was investigated by Karthiga and Narasimhan [1]. Cubic SVM produces accuracy rates with enhanced ROI selection, morphological processes, and curvelet transform. With radiation-free thermal infrared imaging, Yadav and Jadhav [2] is a thermography-based method for early sickness identification. Compared to mammography, machine learning-based thermal scan analysis provides more effective options for non-invasive medical diagnosis. Cauce et al. [3] state that a unique method for diagnosing breast cancer combines clinical and personal data with thermal imaging using a multi-input CNN, significantly improving diagnostic accuracy.Even when mammography performs well, it can cause pain, as noted by Macedo et al. [4]. BC diagnosis is crucial. The assistance of machine learning improves breast thermography accuracy. Abhisheka et al. [5] noted that BC is a worldwide concern, with over 2.1 million diagnoses annually. Early diagnosis is crucial for higher survival rates, and AI-based techniques make this feasible. The study aims to guide future research towards developing automated and reliable models for BC diagnosis.

Breast cancer is a significant worldwide issue, as highlighted by Tsietso et al. [6], which underscores the importance of early detection. Their work proposes a multi-input CADx system that uses several viewpoints of BTs and clinical data, offering a comprehensive approach to BC detection. The results of their study, which show increased sensitivity, suggest a potentially less costly and safer screening technique.Early diagnosis is crucial for BC, as emphasizedby research from Rajinikanth et al. [7]. This paper develops an automated detection approach that achieves high accuracy by using a Decision-Tree classifier with breast thermal pictures.BC requires accurate early detection because it is the leading cause of death for women, as noted by Houssein et al. [8]. This study studies applications of machine and DL to multi-modal medical imaging with an emphasis on trends and issues.Both genders were impacted by Mashekova et al. [9], which calls for early diagnosis using BC. Despite its limitations, thermography has gained popularity due to advancements in technology. AI increases accuracy, but more study and development are required.Early detection is crucial, as noted by Resmini et al. [10]. For screening and diagnosis, thermography is a non-invasive method that shows potential. Additional enhancements are advised since the proposed approach shows potential.

A study by Houssein et al. [11] contributed to the discovery of abnormal temperature fluctuations that might be signs of breast cancer. An enhanced Chimp optimization algorithm (IChOA) performs better than rivalsregarding performance metrics and picture segmentation accuracy. Future research aims to investigate

machine learning hybridization with larger datasets. The rising incidence of cancer, as well as its severe nature and high fatality rate, were noted by Lakshman et al. [12]. With a greater accuracy rate, Random Forest outperforms Support Vector Machine in the identification of cancer. Zeiser et al.'s [13] improved WSI segmentation is made possible by the CNN model DeepBatch. It enhances cellular understanding and has the potential for various cancers. Future goals include pretraining ResNet-50, multimodal exploration, micrometastasis detection, and ethical considerations.Early detection is critical to improving survival rates from BC, which is a global risk to women, according to Rezaei et al. [14]. This study looks at image-based diagnostic methods focusing on 2016–2020. The difficulties include complexity, cost, accuracy, and dependence on people. In the future, addressing challenges with massive data, considering patient information, and combining modalities will be given priority. Liu et al.'s [15] pliable focus Automated metastatic axillary lymph node detection in BC CECT using the VGG19 model pictures produced greater accuracy than earlier methods. The algorithm reduces the work for physicians by providing daily diagnostic help. Future work will focus on three-dimensional analysis, multi-center validation, and better lesion identification.

When comparing DL with ML to predict the recurrence of BC, Krithiga and Geetha's [16] problems with sensitivity and specificity are emphasized. The study assesses several characteristics and methods for histopathology image interpretation, focusing on accuracy improvements and potential big data analytics applications.To identify abnormalities in breast thermograms, Sharma et al. [17] proposed a method based on superpixel-based ROI segmentation and the shearlet transform. Attains a high level of classification accuracy and robustness against incorrect coloring.Bai et al. [18] found that DL changes diagnostic imaging and guarantees technical flexibility when used for BC screening, especially when combined with DBT. For breast cancer thermography, Yousefi et al. [19] presented Deep-SemiNMF and discussed the challenges in basis selection. The model has an impressive categorization capacity, with an accuracy rate of 71.36%. A breast cancer CEUS video classification model with an accuracy and sensitivity of 86.3% was developed by Chen et al. [20] by combining the subject matter knowledge of radiologists.

Advances in medical imaging by Tariq et al. [21] enhance breast cancer early detection. Computer vision and AI classify abnormalities from image modalities, enabling effective computer-aided detection.To segment BC radiotherapy, Bakx et al. [22] tested a DL model that ensures both qualitative and quantitative analysis for therapeutic application.Yadav et al. [23] looked at applying hybrid, ML, and DL approaches for BC detection using mammography datasets and Wisconsin databases. SVM is the most accurate classifier available. Future research may include methodologies such as ensemble machine learning and dimension reduction. A model proposed by Li and Lu [24] uses ResNet101 or MobileNetV2 for breast cancer diagnosis and U-Net for segmentation. Pathologists can swiftly and precisely identify patients thanks to the competitive outcomes. A software developed by Kadry et al. [25] recognizes breast tumors in MRI slices by applying the Slime Mold Algorithm and Watershed Segmentation. Imageperformance measures demonstrate clinicalsignificance.

Applying DL radiology to assess patient therapy in advanced breast cancer enhanced results, as reported by Peng et al. [26]. More datasets and optimal architecture are required to overcome obstacles in ultrasound-based DL. Future research in multimodal analysis is recommended. Real-time communication, ML, and thermography are integrated into the portable infrared imaging system Krishna and George suggested [27] to monitor breast health in remote locations. To construct a more comprehensive CAD system, plans aim to expand the dataset, enhance accessibility, and provide other views.Pereira et al. [28] proposed enhanced attribute selection for breast thermography-based cancer diagnosis. Satisfactory results suggest that generality and accuracy may rise. A minimal database size and age restrictions are a couple of the restrictions. Future goals include expanding the dataset and researching further attributes and methods of selection.Mammography is crucial for the early detection of BC, as noted by Meenalochini and Kumar [29]. It looks at machine learning techniques, focusing on how well they categorize data. Research of a similar nature was discovered in [30].

A method for identifying BC from thermal images was described by Ibrahim et al. [31]. It involved adjusting quick-shift parameters and using the recommended CSSA. The CSSA approach yields strong segmentation results for breast cancer detection, improving accuracy and convergence. Thermal imaging is helpful for early breast cancer detection, as shown by Kakileti et al. [32]. It recommends cascading CNN architecture and displays a high dice index for accurate, view-independent segmentation.The significance of BC and the requirement for early detection methods were highlighted by Husaini et al. [33]. There is potential for combining thermography with AI. Open research questions are offered with review topics.By BC, women were more likely to have Raghavendra et al. [34] developed at critical junctures. It is easier to analyze with thermography. This study examines the accuracy gains from computer-aided diagnosis. Human thermography is a vital medical tool that Farooq and Corcoran [35] improved. The application of IR thermography facilitates the diagnosis of COVID-19 and cancer. The suggested CNN approach yields 80% accuracy in identifying breast tumors.

Singh and colleagues [36] investigated the early detection of BC risk. When used with mammography, IR breast thermography allows for painless, non-invasive diagnosis. Machine learning produces more excellent reliability.BC is a significant cause of mortality that is more common in developing nations because of delayed

diagnosis, as discussed by Kakileti et al. [37]. Future validation of a broader and more diverse population will be made possible by the foundation this study creates.An automated method utilizing statistical features to attain competitiveness for the classification of BTpictures was proposed by Ruiz et al. [38]. The following studies will extract all textural properties from GLCM and investigate CNN, a feature extractor of DL. Mahmood, together with others. [39] emphasized the challenges associated with misdiagnosing breast cancer and advocated for the deployment of efficient DL-based methods. The analysis assesses modality, segmentation, and classification and makes improvements for reliable outcomes. Gomathi et al. [40] introduced the AMF and UAFT to automate the detection of BC. The proposed technique shows promising results in detecting cancer-impacted variations and may be able to diagnose BC, which encourages further research. As the literature review makes clear, there isn't much study on deep learning using encoder-decoder architecture for breast ROI segmentation.

3. PROPOSED FRAMEWORK

Our deep learning system, ROISegNet, was proposed for the automated separation of ROI from breast thermograms. The encoder-decoder architecture, consisting of an encoder with atrous convolution and a specially designed decoder network, is the framework's foundation. Effective segmentation is applied to generate the ROI (breast area) from the provided input breast thermal picture. This aids in the automatic detection of anomalies that may eventually result in breast cancer.Stated differently, thermogram analysis has the potential to identify breast cancer risk early on. The ROISegNet deep learning framework, depicted in Figure 1, is considered significant in this context. An essential architecture component is the atrous convolution method for obtaining dense features for semantic segmentation.

3.1 Dense Feature Extraction

Applying Fully Convolutional DCNNs to semantic segmentation tasks has demonstrated promising results [42, 43]. Aside from the fact that repeated application of max-pooling and striding at progressively higher layers of these networks significantly reduces the spatial resolution of the resulting feature maps, in modern DCNNs, this decrease is often by a factor of 32 in each direction [44, 45]. To recover the spatial resolution, these networks use deconvolutional layers. Instead, we propose to adopt atrous convolution, which was first introduced in [46]. It was previously applied in the context of DCNN by [47]. For efficiently calculating the undecimated wavelet transform. For two-dimensional signals, an intensive convolution is carried out over the output y at each point I; according to Eq. 1, filter w is applied to the feature map input x.

$$y[i] = \sum_k x[i + r.k]w[k] \quad (1)$$

To create a stride convolution, sometimes referred to as a convolution with up-sampled filters, Between each filter value step along each spatial orientation, r - 1 zeros are injected. This is the same as taking r steps to sample the input signal. Through atrous convolution, the rate value may be varied to change the filter's field of vision adaptively. In contrast, Rate r = 1 is an example of ordinary convolution.

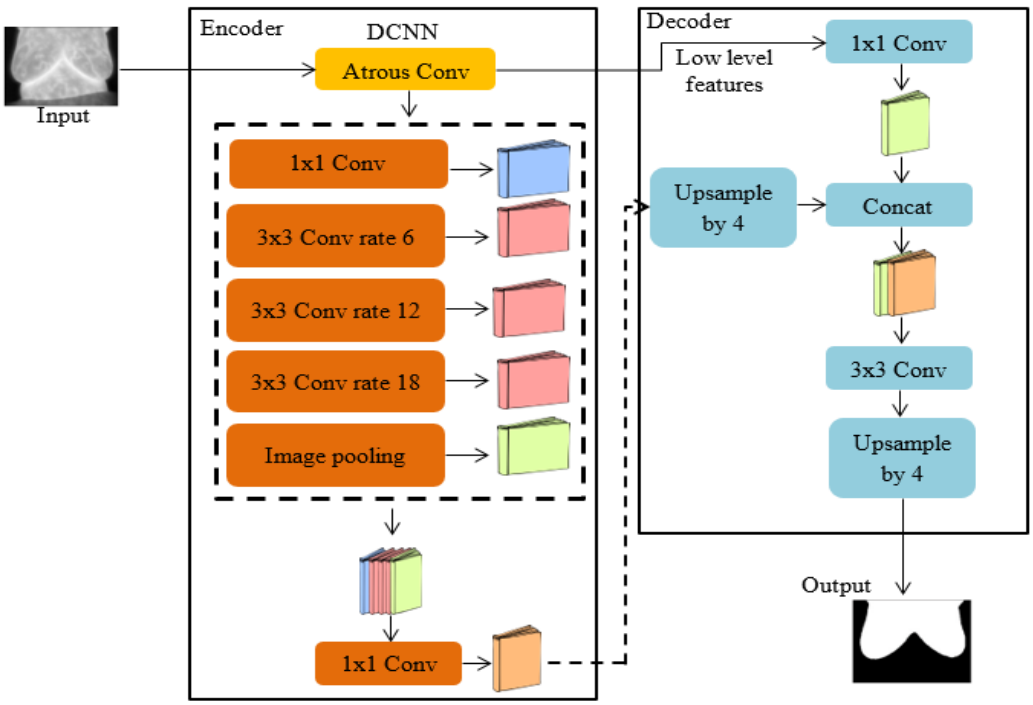

Figure 1: An ROI segmentation system called ROISegNet is suggested for deep learning analysis of breast thermograms.

Furthermore, for fully convolutional networks, atrous convolution gives us control over the density at which feature responses are produced. In this case, the output stride displays the ratio of the input picture's spatial resolution to the final output resolution. For the image classification problem, the output stride of the DCNNs [44], [45] is 32 since the final feature responses (before fully linked layers or global pooling) are 32 times smaller than the input picture dimension. The resolution-reducing stride of the final pooling or convolutional layer is adjusted to 1 to yield up to 16 output strides, doubling the spatial density of the computed feature responses from the DCNNs without causing the signal to become weaker. Use a rate of r = 2 to substitute all subsequent convolutional layers after the atrous convolutional layers. Therefore, we need to learn new abilities to extract richer feature responses. Refer to [48] for further details.

3.2. Atrous Convolution Design

Our first focus is on the construction of cascaded atrous convolution modules. To put it another way, we take the final ResNet block and duplicate it, arranging the copies in a column. Except for the convolution with stride 2 in the last block, which resembles the original ResNet, each block has three 3 × 3 convolutions and a final convolution included. The strategy behind this approach is the faster gathering of long-range data in the deeper blocks, which is made possible by striding. For example, the final small-resolution feature map might provide asummary of the overall feature.The pace at which Atrous convolution is carried out is, therefore, determined by the intended output stride value. However, as we can see, the subsequent stride obliterates detailed information, detrimental to semantic segmentation. We assess our proposed model cascading ResNet blocks up to block 7 with an output stride of 256. This model is evaluated without an atrous convolution included. As we were inspired by multi-grid techniques [49], [50], which use a series of grids with different sizes, we incorporated distinct atrous rates among blocks 4 through 7 in the suggested paradigm. Multi Grid = (r1, r2, r3) specifies the explicit working speeds of the blocks 4 through 7 convolutional layers. The convolutional layer termination speed is obtained by multiplying the unit rate by the applicable rate. In block 4, the three convolutions will have rates such as 2 * (1, 2, 4) = (2, 4, 8), where the output stride is 16, and the multigrid is 1, 2, 4.

3.3. Pyramid Pooling

We revisit the notion of ASPP as presented in [48], whereby four contemporaneous feature maps with atrous convolutions at distinct atrous rates are used. The concept for ASPP was based on the efficiency and dependability of spatial pyramid pooling [51], [52] in resampling characteristics at different scales to identify areas on any given scale. Unlike [48], we incorporate batch normalization into ASPP. ASPP successfully captures data on several scales at varying atrous rates. We find that increasing sample rate decreases with the number of legitimate filter weights (i.e., weights applied to the valid feature region instead of padded zeros). Figure 4 shows how a 65 x 65 feature map may be processed using a 3 × 3 filter with various atrous rates to get the required outcome. When the feature map size approaches the rate value, the 3 × 3 filter degenerates to a simple 1 × 1 filter instead of collecting the complete image context;thus, the only significant filter weight is the center one.To overcome this problem and give the model global context information, we employ image-level features similar to [53]. After bilinearly upsampling, the 256 filters feed image-level properties into a 1 × 1 convolution in the appropriate spatial dimension [54]. After that, the model's final feature map is subjected to normalize and average pooling.

To summarize, the components of our enhanced ASPP are (a) the image-level trait (Fig. 5) and (b) a solitary 1 x 1 feature.Three 3 x 3 convolutions exist with 6, 12, and 18 speeds when the output stride is 16. Each of them has 256 filters and batch normalization. Keep in mind that rates double when the output stride equals 8. Following each feature after branch concatenation, They execute another batch 1 x 1 convolution (standardizing with 256 filters this time) after receiving the final 1 x 1 convolution to produce the logits.

3.4 Interpret Design

Including image-level and ASPP features, the final feature map is the last feature map the encoder computes. The method of convolution that employs kernel k × k and f filters is called [k × k, f]. We rely on ResNet-101 for training and evaluation [55]. The logits are upsampled bilinearly by 16 when the output stride equals 16. With this simplistic decoder architecture, which consists of only bilinear upsampling, performance is improved, and accuracy is 1.2% higher than training without this simple decoder. Our suggested design (Fig. 1) stacks the decoder module and encoder output on top of one another, building on this essential base. To find more potential designs, the decoder module examines three domains. The low-level feature map of the encoder module is first convolutionedto a 1 x 1 more petite size. We are doing a 3 x 3 convolution to yield more accurate segmentation results and, thirdly, choosing the low-level encoder characteristics. More specifically, we use the Conv2 features from the ResNet-101 network backbone and the final feature map from the res2x residual block to assess the impact of the 1 × 1 convolution in the decoder module [3 × 3, 256]. The encoder module operates

more efficiently with 48 or 32 channels in its low-level feature map. Channel reduction is achieved by using [1 × 1, 48].
To illustrate the improved ROI segmentation, the module decoder's 3 x 3 convolutional architecture is then constructed. Two 3x3 convolutions with 256 filters perform better than one or three convolutions if the encoder feature map is encoded using the Conv2 feature map before striding. Reducing the filter count from 256 to 128 or the kernel size from 3 × 3 to 1 x 1. will result in less performance. Using feature maps from both Conv2 and Conv3 by the decoder module is another possibility that is investigated. Once the decoder feature map has been concatenated twice, perform the [3 × 3, 256] procedure to improve each by gradually upsampling it using Conv3 and then Conv2. From that point on, The entire decoding process is comparable to the design of U-Net/SegNet [56]. But there hasn't been any noticeable advancement. Lastly, two [3 × 3, 256] procedures enhance the combination of the encoder feature map and the channel-reduced Conv2 feature map. This uses the remarkably straightforward yet powerful decoder moduleNote that our proposed model's output stride is 4. Due to GPU resource constraints, we haven't looked at richer content output feature maps (output stride < 4).

3.5 Planned Algorithm

To implement our system, we suggested an approach called LbBROIS.Method 1 describes our process and how it works.

Algorithm 1: Intelligent Segmentation of Breast ROI (ISBROI)

Algorithm: Intelligent Segmentation of Breast ROI (ISBROI)
Input: Breast thermogram dataset (DMR-IR) D
Output: Results of segmentation of breast ROI, performance measures P

1. Start
2. (T1, T2)←DivideData(D)
3. Configure RSN model m as in Figure 1
4. Compile m
5. lfeatures←Encoding(T1)
6. dfeatures←EncoderForDenseFeatureExtraction(T1)
7. F←Concatenate(lfeatures, dfeatures)
8. m'←TrainROISegNet(T1)
9. R←PerformSegmentation(m', F', T2)
10. P←EvaluateModel(ground truth, R)
11. Print R
12. Print P
13. End

The input for our method ISBROIis the DMR-IR dataset D. It offers the ability to divide a given dataset into training and testing datasets in order to preprocess it. The constructed and assembled proposed network is called ROISegNet. The encoder consists of an atrous convolution, which may be used to probe convolutional features at various scales at varying rates. It produces low level features and dense features at the picture level. The ultimate feature map, used to train the model, is produced by concatenating the two types of features. Once trained, the model may be saved and applied to thermal image-based semantic segmentation of the breast ROI. The decoder assists the model in fine-tuning segmentation results and object boundaries based on test pictures. Performance statistics are obtained by comparing the suggested model's output

3.6 Method of Evaluation

Figure 2 shows the variety of performance indicators used to evaluate the proposed model based on the confusion matrix

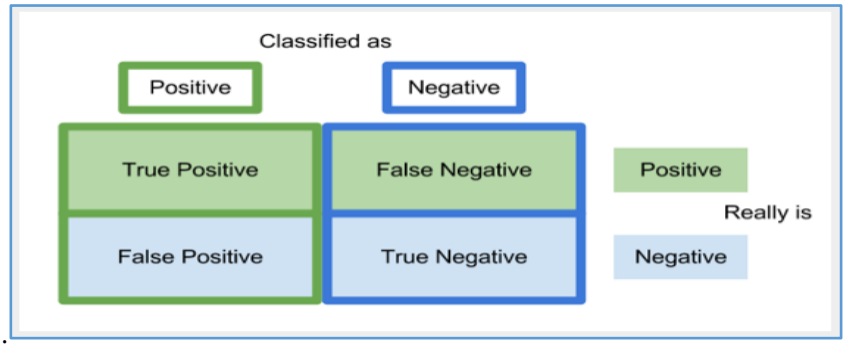

.

Figure 2: Confusing matrix

The percentage of correctly classified pixels that are classed as positive relative to all correctly classified pixels is calculated using precision,which is given in Eq. 2.

$$\text{Precision (p)} = \frac{TP}{TP+FP} \quad (2)$$

Accuracy is a metric that shows the ratio of correctly identified pixels to all of the pixels in an image. This measurement comes from equation 3.

$$\text{Accuracy} = \frac{TP+TN}{TP+TN+FP+FN} \quad (3)$$

Conversely, the union metric intersection (Equation 4) determines the overlap between the ground truth and predicted masks.

$$IoU = \frac{TP}{(TP+FP+FN)} \quad (4)$$

4. EXPERIMENTAL OUTCOMES

Utilizing the DMR-IR benchmark dataset, our framework ROISegNet is assessed [41]. It wasretrieved at the UFF University Hospital. One thousand breast thermograms, divided into evaluation,testing, and validation groups, were employed in this investigation. The samples included both positive and negative breast cancer samples. The suggested framework aims to conduct ROI segmentation to facilitate future breast cancer screening.

4.1 Results

The results of our empirical investigation are shown in this section. Figure 3: An extract from the collection of DMR-IR breast thermograms.

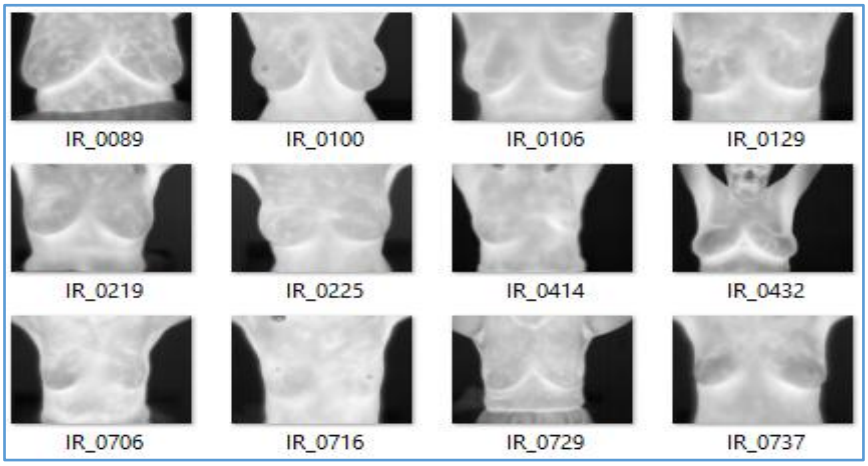

Figure 3: A sample from the collection of DMR breast thermograms

To take advantage of training quality and avoid the overfitting issue, data augmentation is utilized to diversify the data. In Figure 4, an example of the outcomes of the enriched data is shown.

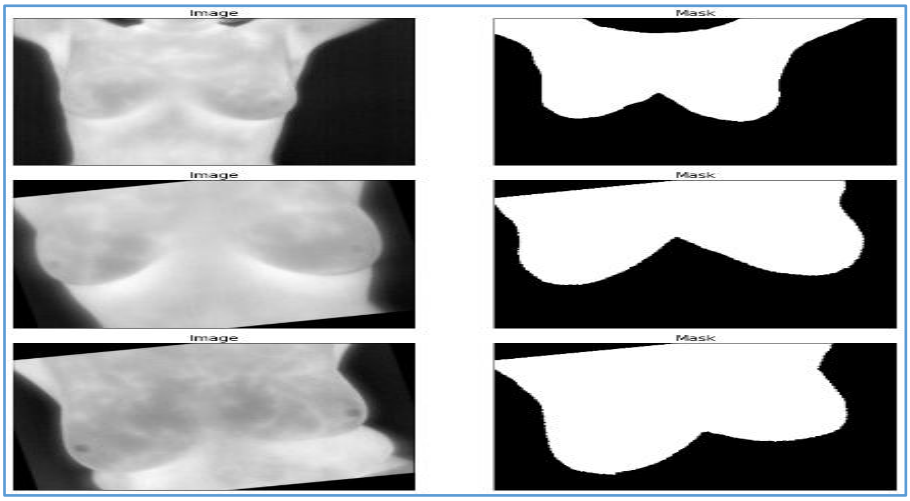

Figure 4: Results of data augmentation

Enhanceddatais provided to train thesuggested model.The architectures of encoders and decoders make up the model, as Figure 1 shows. Finding regions of interest and displaying them is an efficient use of the model. Figure 5 displays the anticipated mark from our experiment, a ground truth mask, and a sample of the original BT.

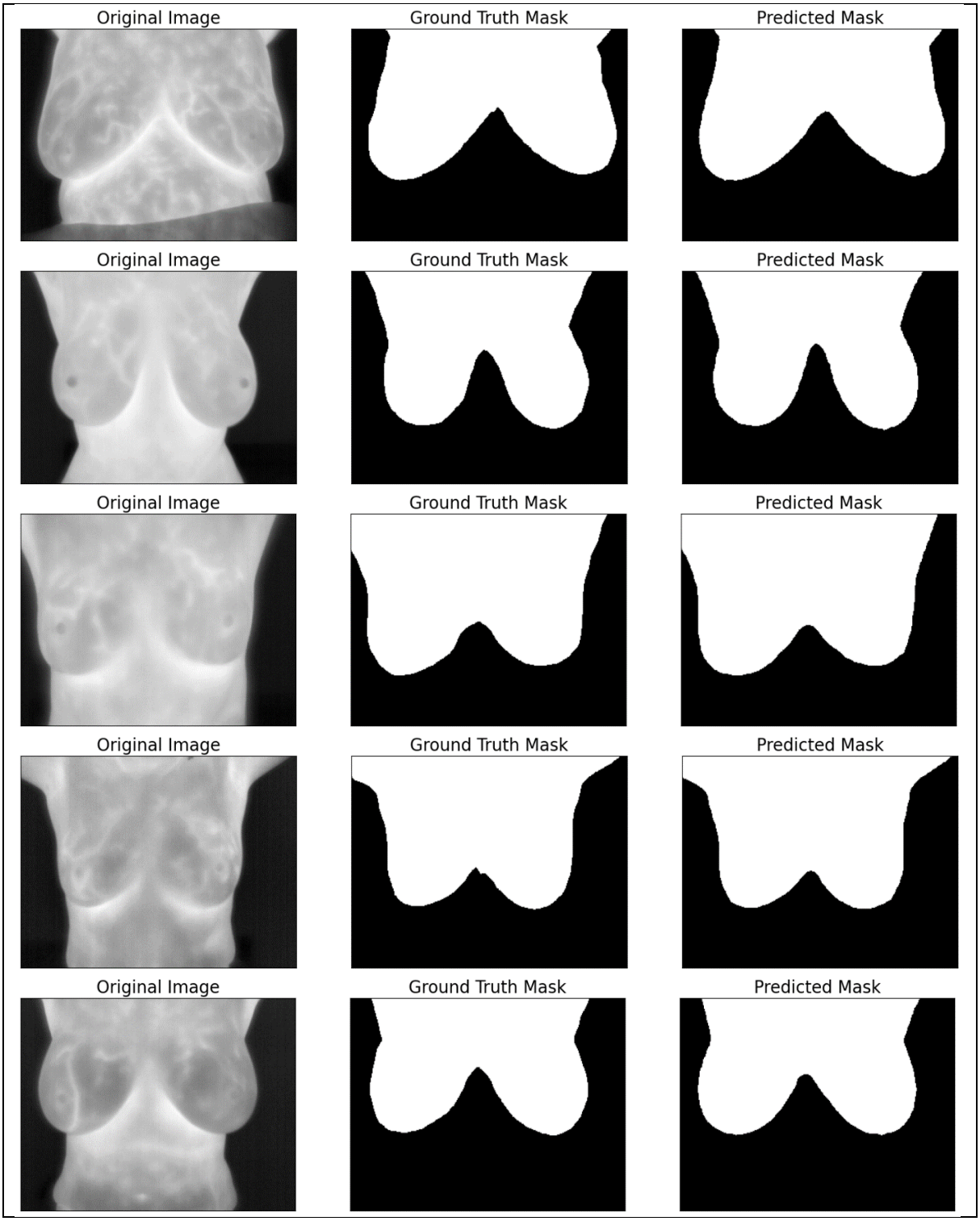

Figure 5:A sample of the experiment's findings showing ROI segmentation

The suggested model can accurately separate breast thermograms according to the ROI segmentation findings. The generated segmented images may be used for BC likelihood detection and classification based on abnormalities found in the ROI. Figure 6 shows the outcomes of ROI-based accurate segmentation.

Figure 6: Result of segmentation

Additional examinations evaluate the suggested model's performance for accuracy, precision, IoU, and dice loss. The proposed model's precise performance is displayed in Figure 7

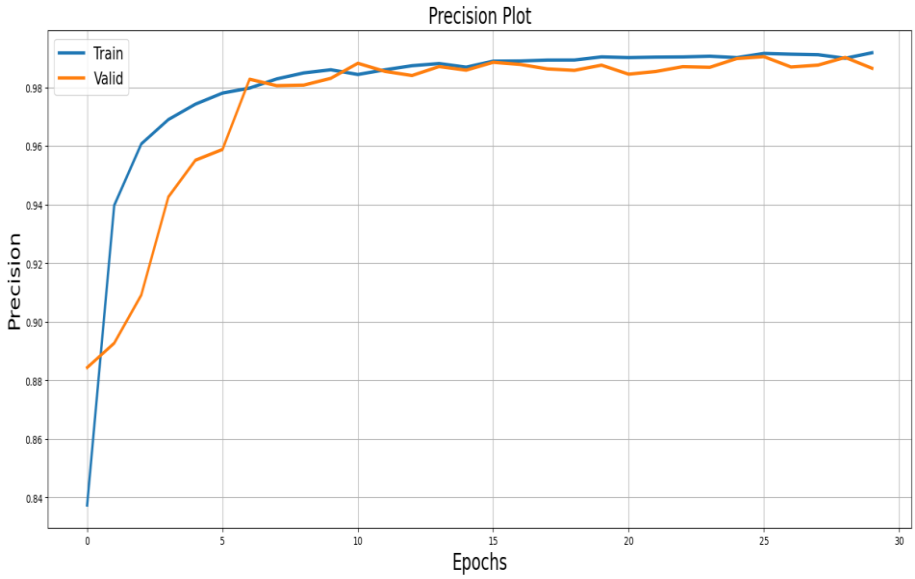

Figure 7: The accuracy with which the proposed model operates

The model's accuracy as a function of epoch count is displayed. The accuracy value steadily increases with the number of epochs. The model has reached its peak accuracy after 30 epochs. The suggested model's level of accuracy is seen in Figure 8.

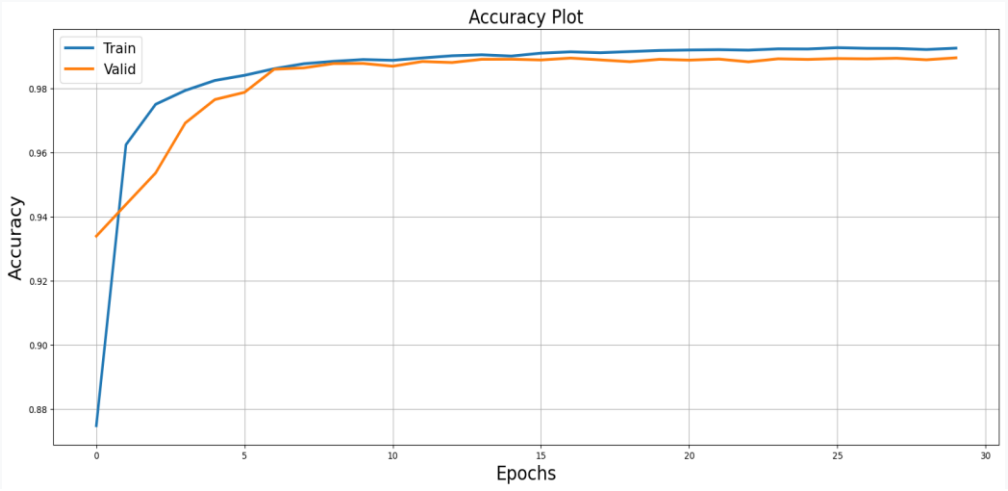

Figure 8: The correctness of the suggested model's performance

The model's accuracy is presented based on the total number of epochs. The accuracy value rises with an increasing number of epochs. The model achieves its highest level of accuracy
after 30 epochs. Figure 9 shows the estimated model's IoU score.

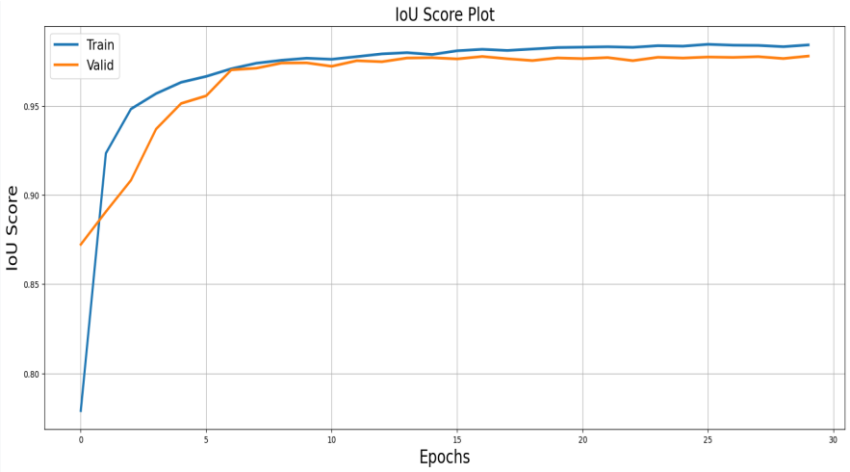

Figure 9: The suggested model's performance as measured by the IoU score

The model's IoU is shown versus the total number of epochs. With an increase in epochs, the IoU value rises gradually. When the model reaches 30 epochs, it has already hit its maximum IoU. The dice loss performance of the proposed model is shown in Figure 10.

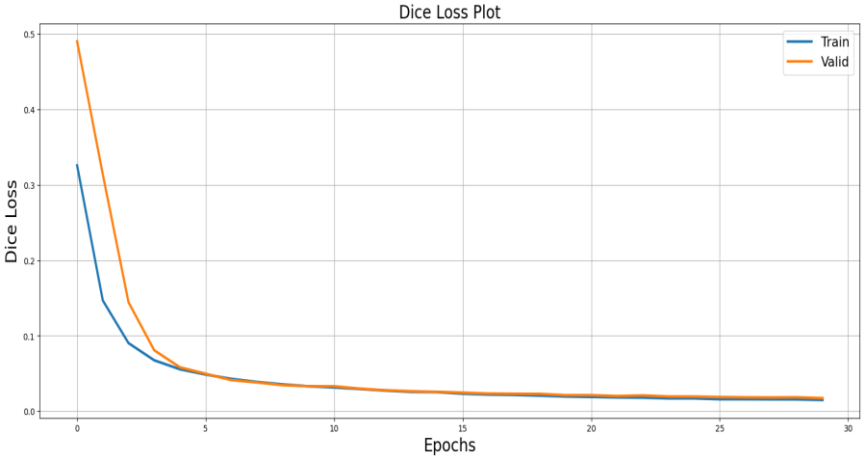

Figure 10: The recommended model's efficacy in terms of dice loss

A graph of the model's dice loss versus epoch count is displayed. A lower dice loss number denotes superior performance. The dice loss value steadily decreases with an increase in epochs. The model finds the least amount of dice loss after 30 epochs. Table 1 presents the convergent performance of the suggested model across all assessment measures.

Metric	Value
Mean Accuracy	0.9863
Mean IoU Score	0.9706
Mean Precision Score	0.9811
Mean Dice Loss	0.0213

Table 1: Displays how well the suggested model performs.

Figure 11 shows the proposed method's performance based on many metrics that assess its suitability for ROI segmentation of brain thermograms.

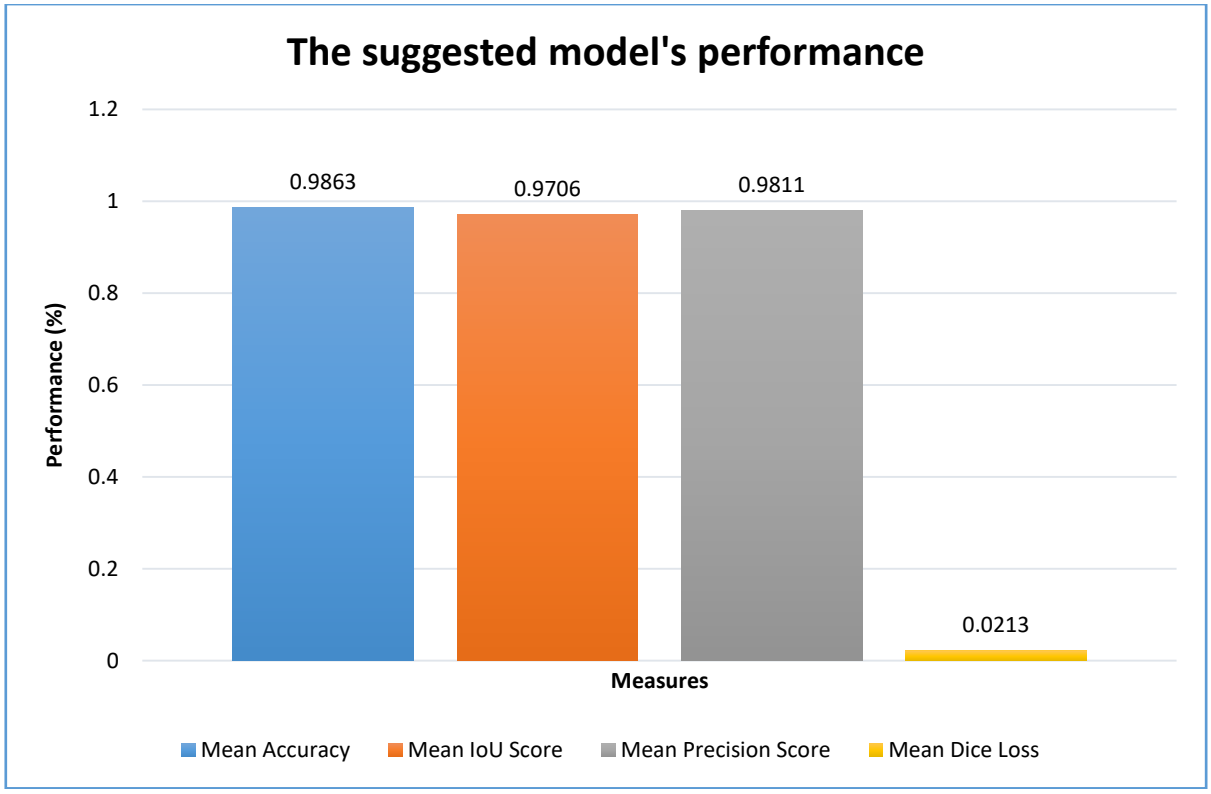

Figure 11: The suggested model's performance

At the last epoch of model execution, the proposed model's mean dice loss was found to be 0.0213. With a mean IoU score of 97.06%, the precision is 98.11% on average,andthe model has an accuracy of 98.63% on average.

4.2 Performance Comparison

We compare our ROISegNet model with other methods currently used for ROI segmentation on breast thermograms. For comparison, we employ models such as Atrous Convolution [55], VGG19 [56], ResNet50 [57], and InceptioV3 [58]. Table 2 presents performance data for multiple models [59].

Table 2: Comparing performance

Segmentation Model	Performance (%)			
	Mean Precision	**Mean IoU Score**	**Mean Accuracy**	**Mean Dice losse**
VGG19	90.4935	89.525	90.9731	0.023
ResNet50	92.3403	91.352	92.8297	0.0226
InceptionV3	94.2248	93.2164	94.7242	0.0221
Atrous Convolution	96.1478	95.1188	96.6574	0.0217
ROISegNet	98.1101	97.0623	98.6312	0.0208

The performance of many different current models is compared with the proposed ROISegNet model. The mean dice loss comparison is displayed in Figure 12.

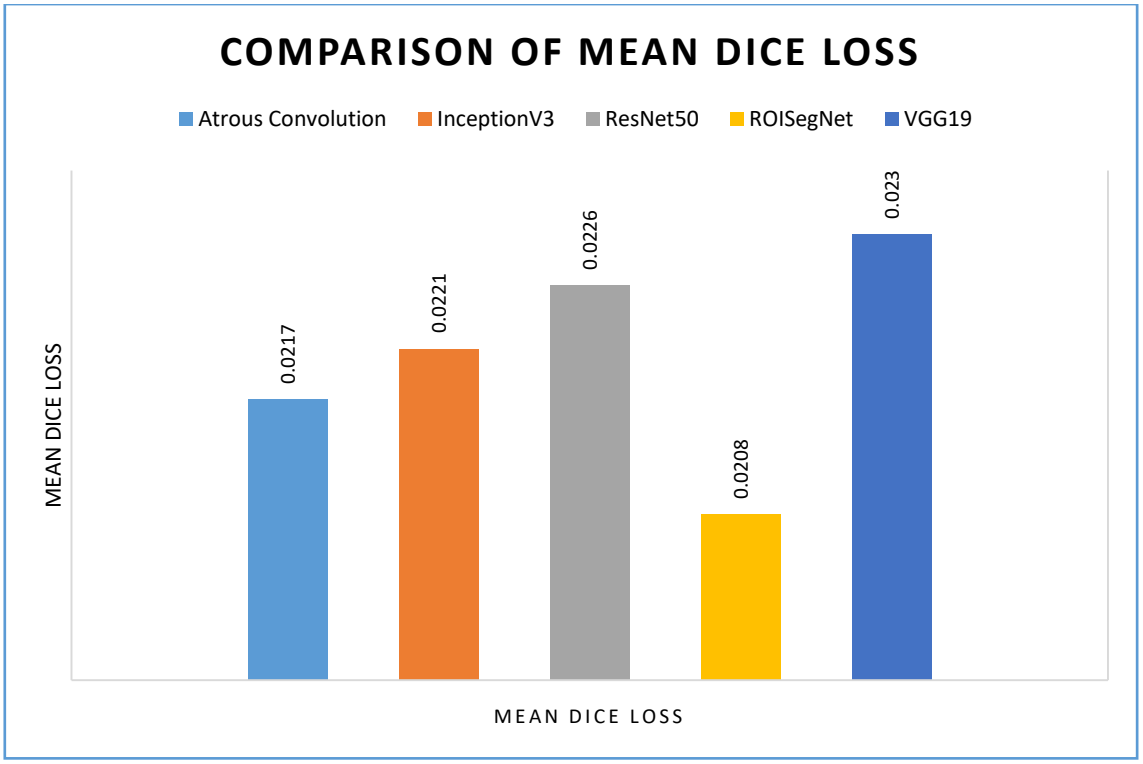

Figure 12: Comparing performance based on average dice loss

The model's average dice loss is 0.023 for VGG19. InceptionV3, Atrous convolution, and ResNet50 had mean dice losses of 0.0226, 0.0221, and 0.0217, respectively. The suggested model, which is 0.0208, has the least dice loss. The results show that the recommended model outperforms the existing models in terms of mean dice loss. In Figure 13, The performance metrics of each model are compared: average precision, average IoU score, and average accuracy [60].

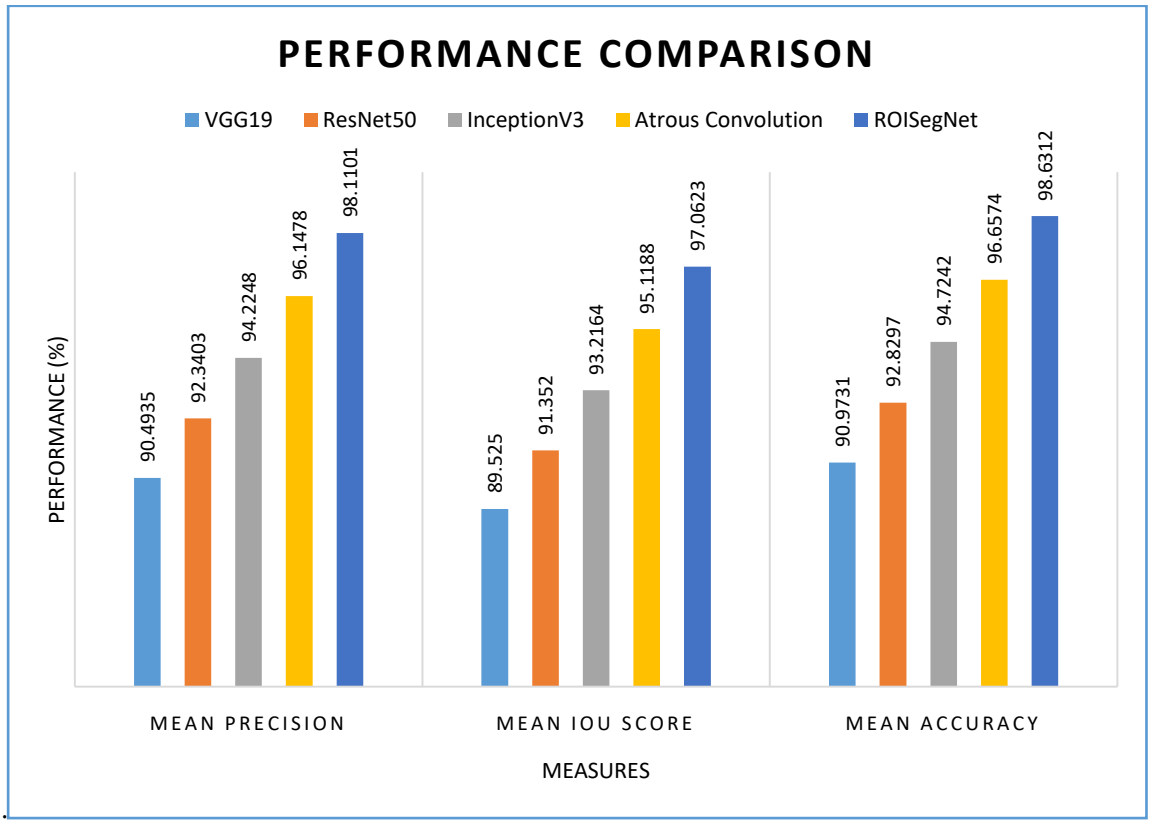

Figure 13:comparing the performance Graph

The mean accuracy values of VGG19, ResNet50, InceptionV3, Atrous Convolution, and ROISegNet are 90.49%, 92.11%, 94.22%, and 96.14%, respectively. The average IoU score for VGG19 is 89.52%, ResNet50 is 91.35%, InceptionV3 is 93.21%, Atrous Convolution is 95.11%, and The average IoU score for ROISegNet is 97.06%. The average accuracy values of VGG19, ResNet50, InceptionV3, Atrous Convolution, and ROISegNet are 90.97%, 92.82%, 94.72%, and 98.63%, respectively. The suggested model performed better in ROI segmentation of breast thermograms than other existing models, according to the experimental results. A decoder module that expands the model based on Atrous Convolution is one of the enhancements that are responsible for ROISegNet's speed boost.

5. CONCLUSION AND FUTURE WORK

Our recommendation was to use ROISegNet, a DL network, to segment the ROI from breast thermogram images automatically. Our method leverages efficiency in semantic segmentation by designing a decoder module and utilizing atrous convolution as part of the encoder. The encoder-decoder architecture, consisting of a customized decoder network and atrous convolution as part of the encoder, is the framework's foundation. The input breast thermal picture is effectively segmented to produce the breast area, or ROI, which aids in the automated identification of anomalies that may eventually result in breast cancer. We proposed an algorithm known as Intelligent Segmentation of Breast ROI (ISBROI). Our empirical investigation using the DMR-IR benchmark dataset showed that ROISegNet achieves the maximum accuracy of 98.63%, outperforming other models like VGG19, ResNet50, InceptionV3, and Atrous Convolution. Due to its concentration on ROI segmentation rather than breast cancer diagnosis, our methodology has a major disadvantage. In order to identify asymptotic patients, we want to build a unique grading system for breast abnormalities in our future study.

REFERENCES

1. R. Karthiga and K. Narasimhan; (2021). Medical imaging technique using curvelet transform and machine learning for the automated diagnosis of breast cancer from thermal image . Pattern Analysis and Applications. http://doi:10.1007/s10044-021-00963-3
2. Samir S. Yadav and Shivajirao M. Jadhav. (2020). Thermal infrared imaging based breast cancer diagnosis using machine learning techniques. Springer. 81, pp.1-19. https://doi.org/10.1007/s11042-020-09600-3
3. Raquel Sánchez-Cauce; Jorge Pérez-Martín and Manuel Luque; (2021). Multi-input convolutional neural network for breast cancer detection using thermal images and clinical data . Computer Methods and Programs in Biomedicine. http://doi:10.1016/j.cmpb.2021.106045
4. Mariana Macedo; Maira Santana; Wellington P. dos Santos; Ronaldo Menezes and Carmelo Bastos-Filho; (2021). Breast cancer diagnosis using thermal image analysis: A data-driven approach based on swarm intelligence and supervised learning for optimized feature selection . Applied Soft Computing. http://doi:10.1016/j.asoc.2021.107533
5. Barsha Abhisheka, Saroj Kumar Biswas and Biswajit Purkayastha. (2023). A comprehensive review on breast cancer detection, classification and segmentation using deep learning. Springer. 30, pp.1-30. https://doi.org/10.1007/s11831-023-09968-z
6. Dennies Tsietso, Abid Yahya, Ravi Samikannu, Muhammad Usman Tariq, Muhammad Babar, Basit Qureshi And Anis Koubaa. (2023). Multi-Input Deep Learning Approach for Breast Cancer Screening Using Thermal Infrared Imaging and Clinical Data. IEEE. 11, pp.52101 - 52116. http://DOI:10.1109/ACCESS.2023.3280422
7. Venkatesan Rajinikanth; Seifedine Kadry; David Taniar; Robertas Damasevicius and Hafiz Tayyab Rauf; (2021). Breast-Cancer Detection using Thermal Images with Marine-Predators-Algorithm Selected Features . 2021 Seventh International conference on Bio Signals, Images, and Instrumentation (ICBSII). http://doi:10.1109/icbsii51839.2021.9445166
8. Houssein, Essam H.; Emam, Marwa M.; Ali, Abdelmgeid A. and Suganthan, Ponnuthurai Nagaratnam (2020). Deep and machine learning techniques for medical imaging-based breast cancer: A comprehensive review. Expert Systems with Applications, 114161–. http://doi:10.1016/j.eswa.2020.114161
9. Aigerim Mashekova, Yong Zhao, Eddie Y.K. Ng, Vasilios Zarikas, Sai Cheong Fok and Olzhas Mukhmetov. (2022). Early detection of the breast cancer using infrared technology – A comprehensive review. Elsevier. 27, pp.1-18. https://doi.org/10.1016/j.tsep.2021.101142
10. Resmini, R., Faria da Silva, L., Medeiros, P. R. T., Araujo, A. S., Muchaluat-Saade, D. C., & Conci, A. (2021). A hybrid methodology for breast screening and cancer diagnosis using thermography. Computers in Biology and Medicine, 135, 104553. http://doi:10.1016/j.compbiomed.2021.104
11. Houssein, E. H., Emam, M. M., & Ali, A. A. (2021). An efficient multilevel thresholding segmentation method for thermography breast cancer imaging based on improved chimp optimization algorithm. Expert Systems with Applications, 185, 115651. http://doi:10.1016/j.eswa.2021.115651

12. Lakshman K; Siddharth B. Dabhade; Y. S. Rode; Karan Dabhade; S. Deshmukh and Ranjan Maheshwari; (2021). Identification of Breast Cancer from Thermal Imaging using SVM and Random Forest Method . 2021 5th International Conference on Trends in Electronics and Informatics (ICOEI). http://doi:10.1109/icoei51242.2021.9452809
13. Zeiser, F. A., da Costa, C. A., Ramos, G. de O., Bohn, H. C., Santos, I., & Roehe, A. V. (2021). DeepBatch: A hybrid deep learning model for interpretable diagnosis of breast cancer in whole-slide images. Expert Systems with Applications, 185, 115586. http://doi:10.1016/j.eswa.2021.115586
14. Zahra Rezaei; (2021). A review on image-based approaches for breast cancer detection, segmentation, and classification . Expert Systems with Applications. http://doi:10.1016/j.eswa.2021.115204
15. Liu, Z., Ni, S., Yang, C., Sun, W., Huang, D., Su, H., … Qin, N. (2021). Axillary lymph node metastasis prediction by contrast-enhanced computed tomography images for breast cancer patients based on deep learning. Computers in Biology and Medicine, 136, 104715. http://doi:10.1016/j.compbiomed.2021.104715
16. Krithiga, R. and Geetha, P. (2020). Breast Cancer Detection, Segmentation and Classification on Histopathology Images Analysis: A Systematic Review. Archives of Computational Methods in Engineering. http://doi:10.1007/s11831-020-09470-w
17. Sharma, R., Sharma, J. B., Maheshwari, R., & Baleanu, D. (2021). Early anomaly prediction in breast thermogram by hybrid model consisting of superpixel segmentation, sparse feature descriptors and extreme learning machine classifier. Biomedical Signal Processing and Control, 70, 103011. http://doi:10.1016/j.bspc.2021.103011
18. Jun Bai; Russell Posner; Tianyu Wang; Clifford Yang and Sheida Nabavi; (2021). Applying deep learning in digital breast tomosynthesis for automatic breast cancer detection: A review . Medical Image Analysis. http://doi:10.1016/j.media.2021.102049
19. Bardia Yousefi; Hossein Memarzadeh Sharifipour and Xavier P. V. Maldague; (2021). A Diagnostic Biomarker for Breast Cancer Screening via Hilbert Embedded Deep Low-Rank Matrix Approximation . IEEE Transactions on Instrumentation and Measurement. http://doi:10.1109/tim.2021.3085956
20. Chen Chen; Yong Wang; Jianwei Niu; Xuefeng Liu; Qingfeng Li and Xuantong Gong; (2021). Domain Knowledge Powered Deep Learning for Breast Cancer Diagnosis Based on Contrast-Enhanced Ultrasound Videos . IEEE Transactions on Medical Imaging. http://doi:10.1109/tmi.2021.3078370
21. Tariq, Mehreen; Iqbal, Sajid; Ayesha, Hareem; Abbas, Ishaq; Ahmad, Khawaja Tehseen and Niazi, Muhammad Farooq Khan (2020). Medical Image based Breast Cancer Diagnosis: State of the Art and Future Directions. Expert Systems with Applications, 114095–. http://doi:10.1016/j.eswa.2020.114095
22. Nienke Bakx, Dorien Rijkaart, Maurice van der Sangen, Jacqueline Theuws , Peter-Paul van der Toorn, An-Sofie Verrijssen, Jorien van der Leer, Joline Mutsaers, Th´er`ese van Nunen, Marjon Reinders, Inge Schuengel, Julia Smits, Els Hagelaar, Dave van Gruijthuijsen, Johanna Bluemink and Coen Hurkmans. (2023). Clinical evaluation of a deep learning segmentation model including manual adjustments afterwards for locally advanced breast cancer. Elsevier. 26, pp.1-6. https://doi.org/10.1016/j.tipsro.2023.100211
23. Rahul Kumar Yadav, Pardeep Singh and Poonam Kashtriya. (2023). Diagnosis of Breast Cancer using Machine Learning Techniques -A Survey. Elsevier. 218, pp.1434-1443. https://doi.org/10.1016/j.procs.2023.01.122
24. Chang Li and Xi Lu; (2021). Computer-Aided Detection Breast Cancer in Whole Slide Image . 2021 International Conference on Computer, Control and Robotics (ICCCR). http://doi:10.1109/icccr49711.2021.9349391
25. Seifedine Kadry; Robertas Damasevicius; David Taniar; Venkatesan Rajinikanth and Isah A. Lawal; (2021). Extraction of Tumour in Breast MRI using Joint Thresholding and Segmentation – A Study . 2021 Seventh International conference on Bio Signals, Images, and Instrumentation (ICBSII). http://doi:10.1109/icbsii51839.2021.9445152
26. Yun Peng, Wei Tang and Xiaoyu Peng. (2023). The study of ultrasonography based on deep learning in breast cancer. Elsevier. 16(4), pp.1-7. https://doi.org/10.1016/j.jrras.2023.100679
27. Sruthi Krishna and Betsy George; (2021). An affordable solution for the recognition of abnormality in breast thermogram . Multimedia Tools and Applications. http://doi:10.1007/s11042-021-11082-w
28. Jessiane M. S. Pereira; Maíra A. Santana; Juliana C. Gomes; Valter Augusto de Freitas Barbosa; Mêuser Jorge Silva Valença; Sidney Marlon Lopes de Lima and Wellington Pinheiro dos Santos; (2021). Feature selection based on dialectics to support breast cancer diagnosis using thermographic images . Research on Biomedical Engineering. http://doi:10.1007/s42600-021-00158-z
29. Meenalochini, G. and Ramkumar, S. (2020). Survey of machine learning algorithms for breast cancer detection using mammogram images. Materials Today: Proceedings, S2214785320364257–. http://doi:10.1016/j.matpr.2020.08.543

30. Saikumar, K., & Rajesh, V. (2023). A Deep Convolutional Neural Network-Based Heart Diagnosis for Smart Healthcare Applications. In Artificial Intelligence for Smart Healthcare (pp. 227-243). Cham: Springer International Publishing.
31. Ibrahim, Abdelhameed; Mohammed, Shaimaa; Ali, Hesham Arafat and Hussein, Sherif E. (2020). Breast Cancer Segmentation from Thermal Images Based on Chaotic Salp Swarm Algorithm. IEEE Access, 1–1. http://doi:10.1109/ACCESS.2020.3007336
32. Kakileti, Siva Teja; Manjunath, Geetha and Madhu, Himanshu J. (2019). 41st Annual International Conference of the IEEE Engineering in Medicine and Biology Society (EMBC) - Cascaded CNN for View Independent Breast Segmentation in Thermal Images. 6294–6297. http://doi:10.1109/embc.2019.8856628
33. Husaini, Mohammed Abdulla Salim Al; Habaebi, Mohamed Hadi; Hameed, Shihab A.; Islam, Md. Rafiqul and Gunawan, Teddy Surya (2020). A Systematic Review of Breast Cancer Detection Using Thermography and Neural Networks. IEEE Access, 8, 208922–208937. http://doi:10.1109/ACCESS.2020.3038817
34. Raghavendra, U; Gudigar, Anjan; Rao, Tejaswi N; Ciaccio, Edward J; Ng, E.Y.K. and Rajendra Acharya, U. (2019). Computer aided diagnosis for the identification of breast cancer using thermogram images: A comprehensive review. Infrared Physics & Technology, 103041–. http://doi:10.1016/j.infrared.2019.103041
35. Srinivasarao, G., Rajesh, V., Saikumar, K., Baza, M., Srivastava, G., & Alsabaan, M. (2023). Cloud-Based LeNet-5 CNN for MRI Brain Tumor Diagnosis and Recognition. Traitement du Signal, 40(4).
36. Singh, Deepika and Singh, Ashutosh Kumar (2020). Role of image thermography in early breast cancer detection- Past, present and future. Computer Methods and Programs in Biomedicine, 183, 105074–. http://doi:10.1016/j.cmpb.2019.105074
37. K. Kishore Raju, Ch.S.V.V.S.N. Murty, Suresh Kumar Kanaparthi, Amdewar Godavari, Kayam Saikumar, "Multi-Dimensional Machine Intelligence Technique on High Computational Data for Bigdata Analytics," SSRG International Journal of Electrical and Electronics Engineering, vol. 11,no. 6, pp. 91-100, 2024. Crossref, https://doi.org/10.14445/23488379/IJEEE-V11I6P110
38. SÃ¡nchez-Ruiz, Daniel; Olmos-Pineda, Ivan and Olvera-LÃ³pez, J. Arturo (2020). Automatic region of interest segmentation for breast thermogram image classification. Pattern Recognition Letters, 135, 72–81. http://doi:10.1016/j.patrec.2020.03.025
39. Mahmood, Tariq; Li, Jianqiang; Pei, Yan; Akhtar, Faheem; Imran, Azhar and Rehman, Khalil ur (2020). A Brief Survey on Breast Cancer Diagnostic with Deep Learning Schemes Using Multi-Image Modalities. IEEE Access, 1–1. http://doi:10.1109/ACCESS.2020.3021343
40. P, Gomathi; C, Muniraj and PS, Periasamy (2020). Breast Thermography Based Unsupervised Anisotropic- Feature Transformation Method For Automatic Breast Cancer Detection. Microprocessors and Microsystems, 103137–.http://doi:10.1016/j.micpro.2020.103137
41. DMR - Database for Mastology Research. Retrieved from http://visual.ic.uff.br/dmi/
42. Y. LeCun, B. Boser, J. S. Denker, D. Henderson, R. E. Howard, W. Hubbard, and L. D. Jackel. Backpropagation applied to handwritten zip code recognition. Neural computation, 1(4):541–551, 1989.
43. P. Sermanet, D. Eigen, X. Zhang, M. Mathieu, R. Fergus, and Y. LeCun. Overfeat: Integrated recognition, localization and detection using convolutional networks. arXiv:1312.6229, 2013.
44. A. Krizhevsky, I. Sutskever, and G. E. Hinton. Imagenet classification with deep convolutional neural networks. In NIPS, 2012.
45. K. Simonyan and A. Zisserman. Very deep convolutional networks for large-scale image recognition. In ICLR, 2015.
46. M. Holschneider, R. Kronland-Martinet, J. Morlet, and P. Tchamitchian. A real-time algorithm for signal analysis with the help of the wavelet transform. In Wavelets: TimeFrequency Methods and Phase Space, pages 289–297. 1989.
47. A. Giusti, D. Ciresan, J. Masci, L. Gambardella, and J. Schmidhuber. Fast image scanning with deep max-pooling convolutional neural networks. In ICIP, 2013.
48. L.-C.Chen,G.Papandreou,I.Kokkinos,K.Murphy,andA.L. Yuille. Deeplab: Semantic image segmentation with deep convolutional nets, atrous convolution, and fully connected crfs. arXiv:1606.00915, 2016.
49. A. Brandt. Multi-level adaptive solutions to boundary-value problems. Mathematics of computation, 31(138):333–390, 1977.
50. D. Terzopoulos. Image analysis using multigrid relaxation methods. TPAMI, (2):129–139, 1986.
51. K. Grauman and T. Darrell. The pyramid match kernel: Discriminative classification with sets of image features. InICCV, 2005.
52. S. Lazebnik, C. Schmid, and J. Ponce. Beyond bags of features: Spatial pyramid matching for recognizing naturalscene categories. In CVPR, 2006.
53. W. Liu, A. Rabinovich, and A. C. Berg. Parsenet: Looking wider to see better. arXiv:1506.04579, 2015.

54. S. Ioffe and C. Szegedy. Batch normalization: Accelerating deep network training by reducing internal covariate shift. arXiv:1502.03167, 2015.
55. Chen, L.C., Papandreou, G., Schroff, F., Adam, H.: Rethinking atrous convolution for semantic image segmentation. arXiv:1706.05587 (2017)
56. Ronneberger, O., Fischer, P., Brox, T.: U-net: Convolutional networks for biomedical image segmentation. In: MICCAI. (2015).
57. Sandeep Wadekar, Dileep Kumar Singh. (2023). A modified convolutional neural network framework for categorizing lung cell histopathological image based on residual n. Elsevier. 4, pp.1-8. [Online]. Available at: https://doi.org/10.1016/j.health.2023.100224
58. Myasar Mundher Adnan, Mohd Shafry Mohd Rahim, Amjad Rehman Khan. (2023). Automated Image Annotation with Novel Features Based on Deep ResNet50-SLT. IEEE. 11, pp.40258-40277. [Online]. Available at: Digital Object Identifier 10.1109/ACCESS.2023.3266296.
59. Liu, Zhiyong; Yang, Chuan; Huang, Jun; Liu, Shaopeng; Zhuo, Yumin; Lu, Xu (2021). Deep learning framework based on integration of S-Mask R-CNN and Inception-v3 for ultrasound image-aided diagnosis of prostate cancer. Future Generation Computer Systems, 114, pp.358–367. doi:10.1016/j.future.2020.08.015.
60. Swarnalatha, T., Supraja, B., Akula, A., Alubady, R., Saikumar, K., & Prasadareddy, P. (2024, July). Simplified Framework for Diagnosis Brain Disease Using Functional Connectivity. In 2024 2nd World Conference on Communication & Computing (WCONF) (pp. 01-06). IEEE.
61. Saikumar, K., & Rajesh, V. (2024). A machine intelligence technique for predicting cardiovascular disease (CVD) using Radiology Dataset. International Journal of System Assurance Engineering and Management, 15(1), 135-151.